

# A new chaotic attractor in a basic multi-strain epidemiological model with temporary cross-immunity

Maíra Aguiar<sup>+</sup> & Nico Stollenwerk<sup>#</sup>

Instituto Gulbenkian de Ciências,  
Apartado 14, 2781-901 Oeiras, Portugal  
and

Faculdade de Ciências and Centro de Matemática  
e Aplicações Fundamentais, Universidade de Lisboa,  
Avenida Prof. Gama Pinto 2, 1649-003 Lisboa, Portugal  
e-mails: <sup>+</sup> maira@igc.gulbenkian.pt and <sup>#</sup> nks22@cam.ac.uk

November 8, 2021

## Abstract

An epidemic multi-strain model with temporary cross-immunity shows chaos, even in a previously unexpected parameter region. Especially dengue fever models with strong enhanced infectivity on secondary infection have previously shown deterministic chaos motivated by experimental findings of antibody-dependent-enhancement (ADE). Including temporary cross-immunity in such models, which is common knowledge among field researchers in dengue, we find a deterministically chaotic attractor in the more realistic parameter region of reduced infectivity on secondary infection ("inverse ADE" parameter region). This is realistic for dengue fever since on second infection people are more likely to be hospitalized, hence do not contribute to the force of infection as much as people with first infection.

Our finding has wider implications beyond dengue in any multi-strain epidemiological systems with altered infectivity upon secondary infection, since we can relax the condition of rather high infectivity on secondary infection previously required for deterministic chaos. For dengue the finding of wide ranges of chaotic attractors open new ways to analysis of existing data sets.

## 1 Introduction

We observe deterministically chaotic attractors [1, 3, 2] like the one in Fig. 1 for a multi-strain model with less infectivity for secondary infection as for the first just by adding temporary cross-immunity to previously existing dengue models.

Either researchers previously focussed in their models on higher infectivity for secondary infection as for the first due to the hypothesized effect of antibody-dependent-enhancement (ADE), which is confirmed in tissue experiments [4, 5], to increase viral load on a secondary infection with a different strain than obtained in the first infection [6, 7]. Or they focussed on temporary cross-immunity versus ADE but again limiting the effect of ADE to increase the contribution of secondary cases to the force of infection [8].

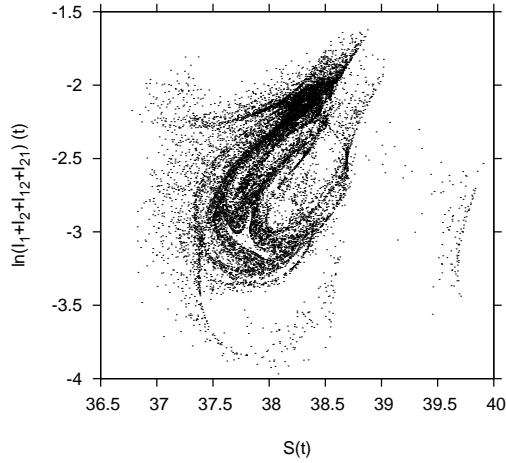


Figure 1: *Deterministically chaotic attractor obtained from a two-strain model with temporary cross-immunity in the "inverse ADE" parameter region of contribution of secondary infection to the overall force of infection. A further description of this graphics will be given in the next sections.*

Our model is a basic two-strain SIR-type model for the host population only slightly refined as opposed to previously suggested models for dengue fever. It is capturing the effective dynamics of the human host population for the dengue virus, keeping effects of the mosquito dynamics (dengue is transmitted by mosquitoes acting as transmission vectors for the virus) or seasonality only in account by the effective parameters in the SIR-type model, but not modelling these mechanisms explicitly. Instead we focus on the multi-strain aspect and its effects on the host population.

This basic model structure allows to generalize our findings to other multi-strain epidemiological systems, but is motivated by modelling dengue fever epidemiology with its peculiar phenomenology.

Dengue is a mosquito-borne infection which in recent years has become a major international public health concern. Two fifths of the world's population is at risk from dengue. The World Health Organization (WHO) estimates there may be 50 million cases of dengue infection worldwide every year. The disease is now endemic in over 100 countries throughout the Americas, South-East Asia, the western Pacific islands, Africa and the Eastern Mediterranean [9].

Dengue fever is transmitted by the female domestic mosquito *Aedes aegypti*, although *Ae. albopictus* and *Ae. polynesiensis* can also act as vector [10]. Virus transmission in its simplest form involves the ingestion of viremic blood by

mosquitoes and passage to a second susceptible human host. The mosquito becomes infected when taking a blood meal from a viraemic person. After an extrinsic incubation period, the mosquito becomes infective and remains so during its entire life span [12].

As the blood meal stimulates ovoposition, which undergoes at least one, often more, reproductive cycles there is an opportunity of vertical transmission to the eggs, passing the virus to the next generation of mosquitoes [13, 11]. In a dry state, eggs survive for very long periods and the virus can persist until the subsequent rainy season [14].

Dengue is caused by four antigenically distinct single-strand positive-polarity RNA viruses, designated dengue types 1, 2, 3, and 4, and belonging to the family Flaviviridae [9]. Infection by one serotype confers life-long immunity to only that serotype and temporary cross-immunity to other serotypes exists. It lasts from three to nine months, when the antibody levels created during the response to that infection would be enough to protect against infection by a different but related serotype [17, 8].

Two forms of the disease exist: dengue fever (DF) or classic dengue, often benign, and dengue hemorrhagic fever (DHF), which may evolve towards a severe form known as dengue shock syndrome (DSS) [15]. Without proper treatment DHF case fatality rates can exceed 20% [9]. DF is characterized by headache, retro-orbital pain, myalgia, arthralgia, rash, leukopenia, and mild thrombocytopenia. The symptoms resolve after 2–7 days. DHF is a potentially deadly complication that is characterized by high fever and haemorrhagic phenomena. DHF develops rapidly, usually over a period of hours, and resolves within 1–2 days in patients who receive appropriate fluid resuscitation. Otherwise, it can quickly progress to shock [16].

There are indeed pre-existing antibodies to previous dengue virus that cannot neutralize but rather enhance infection *in vitro*, a process described as antibody-dependent enhancement. Epidemiological studies support the association of DHF and DSS with secondary dengue infection. Halstead [9, 4, 5] found that DHF and DSS were 15-80 times more likely in secondary than in primary infections and were positively associated with pre-existing dengue-virus-specific antibodies. However, there is no animal model of DHF and DSS, and the causal relationship between ADE and severe disease remains unverified [16].

There is no specific treatment for dengue. A vaccine against dengue is not yet available, since it would have to simulate a protective immune response to all four serotypes [18].

Mathematical models describing the transmission of dengue viruses appeared in the literature as early as 1970 [19]. More recently modelling attention has focussed on including ADE as due to higher viral load of hosts on secondary infection than on the first, hence a higher contribution to the force of infection of each strain, reporting deterministically chaotic attractors [6] and chaos desynchronization [7] to explain the co-existence of the known four dengue viral strains. Temporary cross-immunity against all strains after a first infection has been included in mathematical models as well [8], but to our knowledge, no systematic investigation of the attractor structures of simple two-strain models with dengue-realistic temporary cross-immunity and decreased contribution of

secondary infection to the force of infection, due to severity of infection with a second strain and eventual hospitalization, has been performed so far.

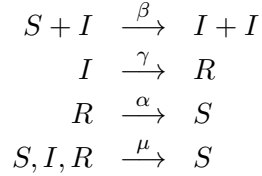
Our finding of chaotic attractors in this parameter region thus indicate that deterministic chaos is wider present than previously expected in multi-strain models. For such scenarios new tools of non-linear data analysis like Takens' embedding are available [20, 21], and allow to obtain topological information (fixed points, periodic orbits and the nature of chaotic attractors) about the whole multi-strain epidemiological system from time series of overall infecteds only, not needing any single strain data sets.

In the next section we present the two-strain model and give the deterministic mean field version of it. We then analyze the deterministic ODE-model in various parameter regions in its attractor structure.

## 2 The basic epidemic model

Multi-strain dynamics are modelled with SIR-type models, dividing the host population into susceptible, infected and recovered individuals.

In the simple SIR epidemics without strain structure of the pathogens we have the following reaction scheme for the possible transitions from one to another state



for a host population of  $N$  individuals, with contact and infection rate  $\beta$ , recovery rate  $\gamma$  and temporary immunity rate  $\alpha$ . Demography is denoted in the last reaction as exits from all classes  $S$ ,  $I$  and  $R$  with rate  $\mu$  to the new born susceptibles.

To include population noise stochastic models are investigated. For state vectors  $\underline{n}$ , here for the SIR-model  $\underline{n} = (S, I, R)$ , the master equation [22] reads

$$\frac{dp(\underline{n})}{dt} = \sum_{\tilde{\underline{n}} \neq \underline{n}} w_{\underline{n}, \tilde{\underline{n}}} p(\tilde{\underline{n}}) - \sum_{\tilde{\underline{n}} \neq \underline{n}} w_{\tilde{\underline{n}}, \underline{n}} p(\underline{n}) \quad (1)$$

with transition rates  $w_{\underline{n}, \tilde{\underline{n}}}$  given by the following expressions

$$\begin{aligned} w_{(S+1, I, R-1), (S, I, R)} &= \alpha \cdot R \\ w_{(S-1, I+1, R), (S, I, R)} &= \beta \cdot \frac{I}{N} S \\ w_{(S, I-1, R+1), (S, I, R)} &= \gamma \cdot I \end{aligned} \quad (2)$$

from which the rates  $w_{\underline{n}, \tilde{\underline{n}}}$  follow immediately as

$$\begin{aligned} w_{(S, I, R), (S-1, I, R+1)} &= \alpha \cdot (R+1) \\ w_{(S, I, R), (S+1, I-1, R)} &= \beta \cdot \frac{I-1}{N} (S+1) \\ w_{(S, I, R), (S, I+1, R-1)} &= \gamma \cdot (I+1) \quad . \end{aligned} \quad (3)$$

In addition we have the transitions for the demography with rate  $\mu$ , e.g. for the transition from recovered to susceptibles  $w_{(S+1,I,R-1),(S,I,R)} = \mu \cdot R$ . This formulation defines the stochastic process completely to capture demographic noise and will be the basis for the multi-strain model to be described in the following.

The above mentioned deterministic ODE model describes in mean field approximation the dynamics of the mean values, e.g.

$$\langle I \rangle := \sum_{I=0}^N I p(S, I, R) \quad . \quad (4)$$

The dynamics for the mean value is then given by inserting the master equation

$$\frac{d}{dt} \langle I \rangle = \frac{\beta}{N} \cdot \langle I \cdot S \rangle - (\gamma + \mu) \cdot \langle I \rangle \approx \frac{\beta}{N} \cdot \langle I \rangle \cdot \langle S \rangle - (\gamma + \mu) \cdot \langle I \rangle \quad (5)$$

with the mean field approximation  $\langle I \cdot S \rangle \approx \langle I \rangle \cdot \langle S \rangle$ . Carried out for all mean values  $\langle S \rangle$ ,  $\langle I \rangle$  and  $\langle R \rangle$  gives a closed ODE system for the SIR dynamics, which is a deterministic system in the sense that initial values determine the time course of the system for all times. The mean field ODE system reads, now omitting the brackets for mean values,

$$\begin{aligned} \frac{dS}{dt} &= \alpha R - \frac{\beta}{N} \cdot I \cdot S + \mu(N - S) \\ \frac{dI}{dt} &= \frac{\beta}{N} \cdot I \cdot S - \gamma I - \mu I \\ \frac{dR}{dt} &= \gamma I - \alpha R - \mu R \end{aligned} \quad (6)$$

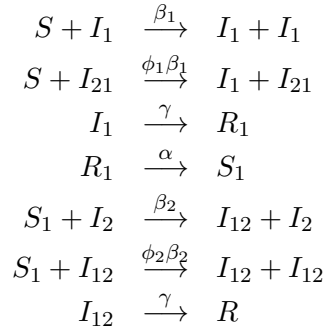
and has only fixed points as possible stationary solutions, i.e. attractors. Transients under certain parameter values oscillate into the fixed point, hence can be already more complex than the final attractor. Stochastic versions of such models with only fixed points possible as attractors but oscillating transients are reported to also show stabilization of the oscillations due to population noise [23, 24]. So the deterministic mean field ODE models with their attractors give rather the minimal complexity caused by the model structure.

## 2.1 Basic two-strain model

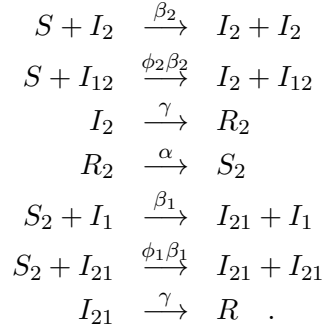
For two strains, 1 and 2, we have the following SIR-type model, now labelling the SIR classes for the hosts that have seen the individual strains. Susceptibles to both strains (S) get infected with strain 1 ( $I_1$ ) or strain 2 ( $I_2$ ), with force of infection  $\beta_1$  and  $\beta_2$  respectively. They recover from infection with strain 1 (becoming  $R_1$ ) or from strain 2 (becoming  $R_2$ ), with recovery rate  $\gamma$ . In this recovered class, people have full immunity against the strain that they were exposed to and infected, and also, temporary immunity against the other strain (called period of temporary cross-immunity). After this, with rate  $\alpha$ , they enter again in the susceptible classes ( $S_1$  respectively  $S_2$ ), where the index represents the first infective strain. Now,  $S_1$  can be reinfected with strain 2

( $I_{12}$ ) and  $S_2$  can be reinfected with strain 1 ( $I_{12}$ ), with infection rates  $\phi_2\beta_2$  and  $\phi_1\beta_1$ . The parameter  $\phi$  in our model acts as "inverse ADE parameter", decreasing the infectivity of secondary infection, where people are more likely to be hospitalized because of the severity of the disease (DHF), do not contributing to the force of infection as much as people with first infection do. Finally,  $I_{12}$  and  $I_{12}$  go to the recovered class (R), immune against all strains. We include demography of the host population by denoting the birth and death rate by  $\mu$ , assuming constant population size  $N$ .

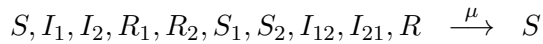
In the following reaction scheme we describe the transitions for first infection with strain 1 and secondary infection with strain 2



and for the reverse process, where the first infection is caused by strain 2 and the secondary infection is caused by strain 1.



The demographic transitions are



defining the system of two strains completely.

The stochastic version is now in complete analogy to the previous SIR model, and we can calculate the mean field equations (or simply read it off from the reaction scheme directly).

The mean field ODE system for the two strain epidemiological system is

$$\begin{aligned}
\frac{dS}{dt} &= -\frac{\beta_1}{N}S(I_1 + \phi_1 I_{21}) - \frac{\beta_2}{N}S(I_2 + \phi_2 I_{12}) + \mu(N - S) \\
\frac{dI_1}{dt} &= \frac{\beta_1}{N}S(I_1 + \phi_1 I_{21}) - (\gamma + \mu)I_1 \\
\frac{dI_2}{dt} &= \frac{\beta_2}{N}S(I_2 + \phi_2 I_{12}) - (\gamma + \mu)I_2 \\
\frac{dR_1}{dt} &= \gamma I_1 - (\alpha + \mu)R_1 \\
\frac{dR_2}{dt} &= \gamma I_2 - (\alpha + \mu)R_2 \\
\frac{dS_1}{dt} &= -\frac{\beta_2}{N}S_1(I_2 + \phi_2 I_{12}) + \alpha R_1 - \mu S_1 \\
\frac{dS_2}{dt} &= -\frac{\beta_1}{N}S_2(I_1 + \phi_1 I_{21}) + \alpha R_2 - \mu S_2 \\
\frac{dI_{12}}{dt} &= \frac{\beta_2}{N}S_1(I_2 + \phi_2 I_{12}) - (\gamma + \mu)I_{1,2} \\
\frac{dI_{21}}{dt} &= \frac{\beta_1}{N}S_2(I_1 + \phi_1 I_{21}) - (\gamma + \mu)I_{21} \\
\frac{dR}{dt} &= \gamma(I_{12} + I_{21}) - \mu R
\end{aligned} \tag{7}$$

We consider  $\phi_1 = \phi_2 = \phi$ ,  $\beta_1 = \beta_2 = \beta$  for the moment, hence no epidemiological asymmetry between the strains.

To take biological information from experiences in dengue into account we fix the transition rates of the model as far as is known, and only will vary the unknown parameters  $\phi$  and eventually  $\alpha$ . Future work will have to also adjust the other parameters better to describe actual data of dengue cases. The parameter values are, if not otherwise explicitly stated,  $\mu = 1/65 \text{ years}$ ,  $\gamma = 52y^{-1}$ ,  $\beta = 2 \cdot \gamma$  and  $\alpha = 2y^{-1}$ . For the chaotic attractors we take the exemplaric values  $\phi = 0.7$  and  $\phi = 2.7$ . We will also vary  $\phi$  continuously to obtain bifurcation diagrams [3, 2].

### 3 Analysis of the multi-strain model with temporary cross-immunity

We will first look at time series simulations of the present model, Eq. system (7), and from there we performed a detailed analysis of chaos, investigating state space plots for various values for  $\phi$ , observing a rich structure of attractors from fixed points to bifurcating limit cycles and chaotic attractors. Finally, we

will show whole bifurcation diagrams for a systematic analysis for the entire parameter region of  $\phi$  for various values of the temporary cross-immunity  $\alpha$ .

### 3.1 Time series for $\phi > 1$

In order to classify the dynamic pattern of the model for various parameters we discard long transients which would carry some information of the initial conditions. So we neglect the first 2000 years in the following simulations. We first simulate time series for  $\phi > 1$ , see Fig. 2 and Fig. 3.

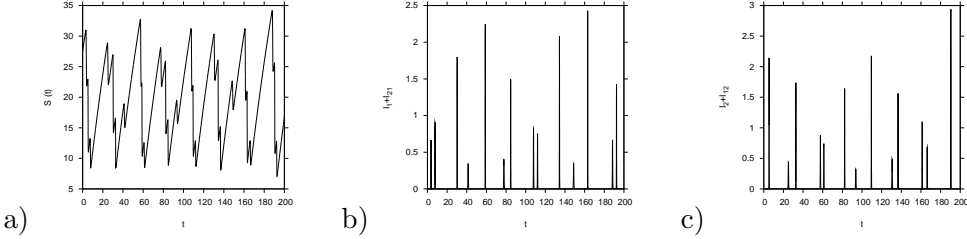


Figure 2: For  $\phi = 2.7$ , time series simulations of a) the susceptibles  $S$ , b) the at the moment infected with strain 1 ( $I_1 + I_{21}$ ), c) the at the moment infected with strain 2 ( $I_2 + I_{12}$ ). Temporary cross-immunity is assumed to be  $\alpha = 2$ . The absolute numbers on the y-axes indicate percentage ( $N = 100$ ).

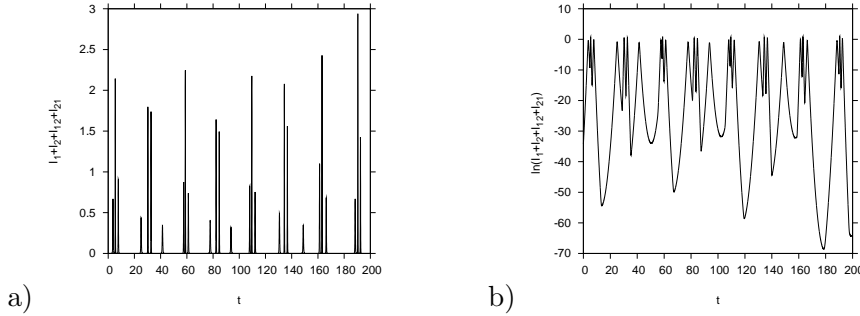


Figure 3: Using the same parameter values above, In a) we plot the time series of the total number of infected  $I := I_1 + I_2 + I_{12} + I_{21}$ , and in b) time series of the logarithm of the overall infected ( $\ln(I)$ ), for the same time interval. Very deep troughs are observed for these parameter values.

However, also the transients reflect the dynamic behaviour of the system under the present parameter values. Spiraling into a fixed point often indicates a nearby periodic orbit. Irregular transients indicate chaotic behaviour in neighbouring parameter regions etc. Hence, even if dengue fever would be evolutionarily younger than the mentioned 2000 years of transient, the observed pattern would still give information about the dynamics of the system. Also the stochastic version of this deterministic mean field model would be rather more complex than the attractor classification and not simpler [23, 24], of course besides extinction due to population fluctuations for eventually very low numbers of infected.



Rather low troughs are observed for the total number of infected leading to unrealistically low numbers of infected on average in low epidemic times. The present deterministic model can be interpreted as a mean field model for stochastic models capturing the effect of population noise e.g. in terms of master equations as mentioned before [22]. The ODE solutions are then the mean values of such stochastic models. Population fluctuations would in the present case drive always the system to extinction.

### 3.2 Time series for $\phi < 1$

Investigating time series for  $\phi < 1$ , as would be realistic for dengue fever due to more severe disease upon reinfection, hence larger chance of being hospitalized, also indicates more complicated dynamic behaviour than just simple fixed point or limit cycles. Discarding the first 2000 years, see Fig. 4 and Fig. 5.

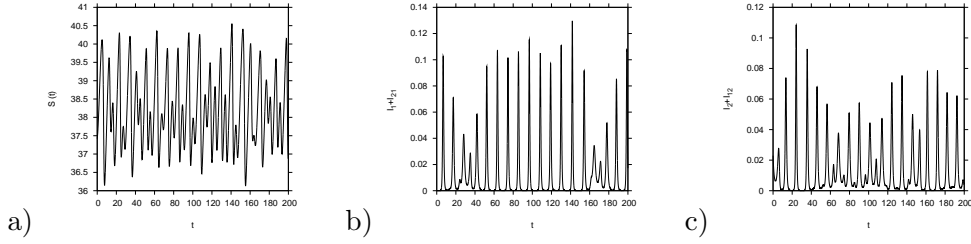


Figure 4: For  $\alpha = 2$  and  $\phi = 0.7$ , time series simulations of a) the susceptibles  $S$ , b) the at the moment infected with strain 1 ( $I_1 + I_{21}$ ), and c) the at the moment infected with strain 2 ( $I_2 + I_{12}$ ).

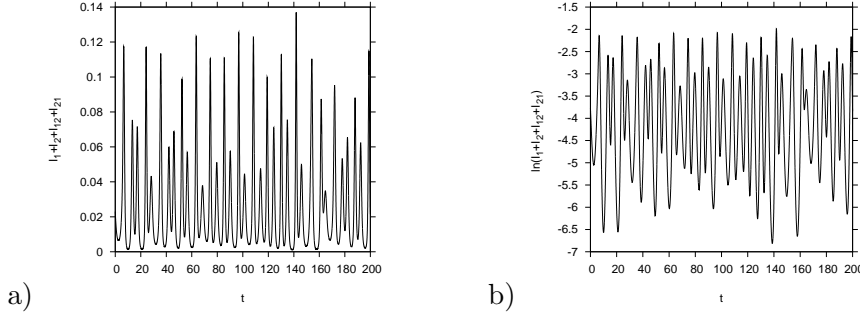


Figure 5: Using the same parameter values above, in a) we plot the time series of the total number of infected  $I := I_1 + I_2 + I_{12} + I_{21}$ , and in b) time series of the logarithm of the overall infected ( $\ln(I)$ ), for the same time interval.

For  $\phi < 1$  the number of infected stays quite away from zero, avoiding the chance of extinction in stochastic systems with reasonable system size. In Fig. 3 b) the logarithm of total infected goes as low as  $-70$ , when  $\phi > 1$ . For  $\phi < 1$ , see Fig. 5 b) the logarithm of total infected does not pass below  $-7$ .

This encourages to also look closer to the parameter region of  $\phi < 1$ , the region of "inverse ADE", i.e. when dengue patients with severe disease because

of the ADE phenomenon contribute less to the force of infection due to possible hospitalization, and not more, as previous models suggested.

### 3.3 State space plots

In Fig. 6 we plot 500 years of dynamics to clearly observe the dynamic patterns present.

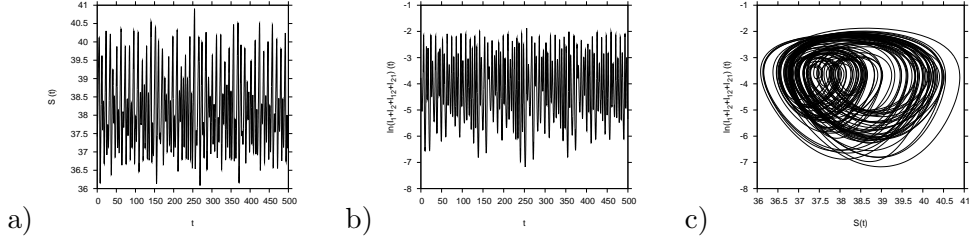


Figure 6: For  $\alpha = 2$  and  $\phi = 0.7$ , we plot in a) the time series of the susceptibles after discarding a long transient (here 2000 years), and in b) the time series of the logarithm of the overall infected,  $I := I_1 + I_2 + I_{12} + I_{21}$  for the same time interval. In c) State space plot of the number of susceptibles versus logarithm of the overall infected, as show from their time series in Fig. 6 a) and b), finding a chaotic attractor. Parameters:  $\alpha = 2$ ,  $\phi = 0.7$ .

We now plot the total number of infected with one strain versus the total number of infected with the other strain. In case of synchronicity of the two strains we would expect the system to stay closer to the main diagonal of the plot, whereas for anti-synchronicity it would mainly stay near the off-diagonal. The observed pattern is more supporting anti-synchronicity, but near-synchronicity can also be observed at times (see Fig. 7). For quantification of these effects of chaos synchronization or chaos desynchronization applied to dengue models see Schwartz *et al.* [7].

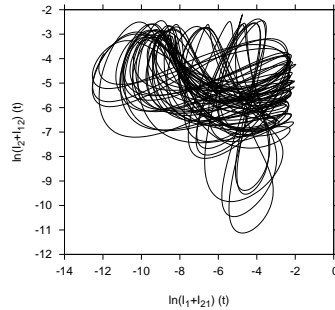


Figure 7: State space plot of the logarithmic number of infected with strain 1 versus the ones with strain 2. Parameters:  $\alpha = 2$ ,  $\phi = 0.7$ .

In the further analysis we will investigate the state space plots in terms of the variables  $S$  and the logarithm of  $I := I_1 + I_2 + I_{12} + I_{21}$ , since dengue notification data often do not distinguish between the circulating strains, hence

the total number of infected  $I$ , whereas the susceptible class  $S$  is  $N$  minus every host who ever has experienced an infection.

In eventual data analysis the method of delay coordinates even allows to only work with one time series of  $I$ , and analysing  $I(t)$ ,  $I(t + \tau)$  etc. with a time delay  $\tau$  [20, 25].

### 3.4 Bifurcations of limit cycles when changing $\phi$

The state space plots for various values of  $\phi$  show bifurcations from fixed point behaviour to limit cycles, which then bifurcate into double-limit cycles etc.,

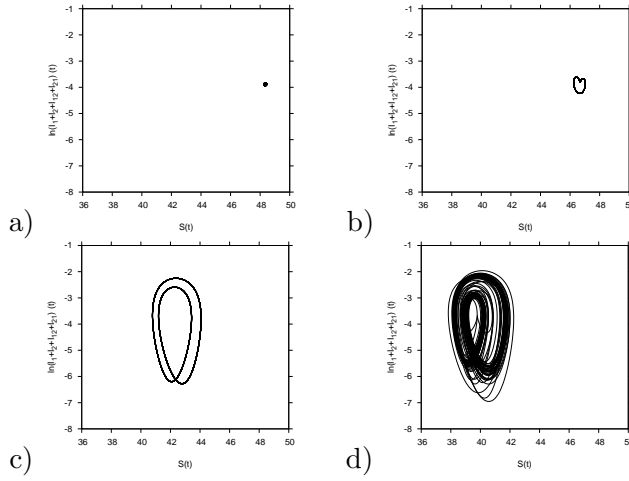


Figure 8: *Attractors for various values of  $\phi < 1$ : a) fixed point for  $\phi = 0.1$ , b) limit cycle for  $\phi = 0.2$ , c) bifurcating limit cycle for  $\phi = 0.45$ , d) chaotic attractor for  $\phi = 0.6$ .*

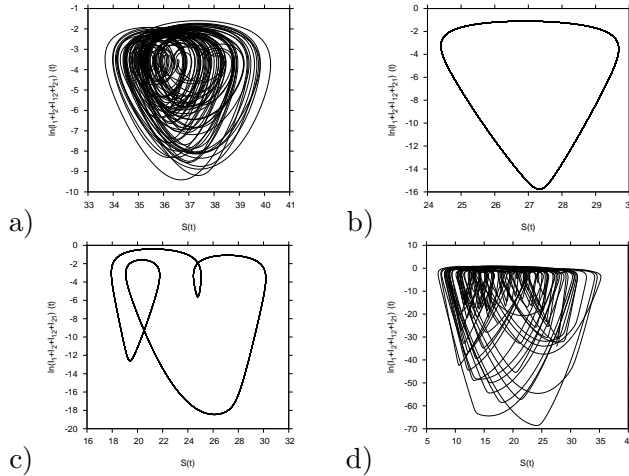


Figure 9: *Attractors for various values of  $\phi$  around 1 and larger: a) chaotic attractor for  $\phi = 0.8$ , b) limit cycle for  $\phi = 1.5$ , c) more complicated limit cycle for  $\phi = 1.9$ , d) chaotic attractor for  $\phi = 2.7$ .*

until completely irregular behaviour, which is the fingerprint of deterministic chaos. See Fig. 8 and Fig. 9.

Looking for higher values of  $\phi$ , than just towards the first chaos window, shows that the chaotic attractor becomes unstable again, just leaving simple limit cycles as attractors for large parameter regions beyond of  $\phi = 1$ . Only for much higher values of  $\phi \gg 1$ , another chaotic attractor appears, the so-called ADE chaotic attractor [6, 7].

### 3.5 Map of maxima of $I$ in state space

We also investigate maxima maps in order to classify the dynamics for various parameter values. see Fig. 10 and Fig. 11.

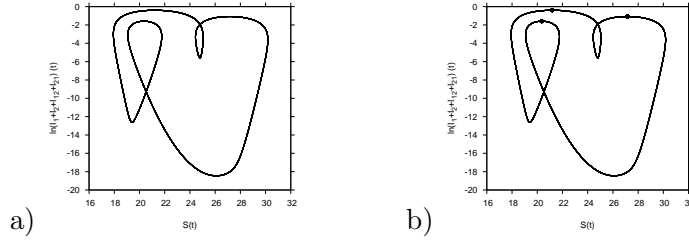


Figure 10: a) Limit cycle for  $\phi = 1.9$ , b) The dots indicate the local maxima calculated for the twisted limit cycle of a). The three dots characterize the three limit cycle. Parameters:  $\alpha = 2$ ,  $\phi = 1.9$ .

We plot for the time  $t_{max}$ , at which the total number of infected  $I(t) := I_1 + I_2 + I_{12} + I_{21}$  has a local maximum, the number of infected at that time  $\ln(I(t_{max}))$  and for the same time value the susceptibles  $S(t_{max})$ . In this way we obtain a maxima map.

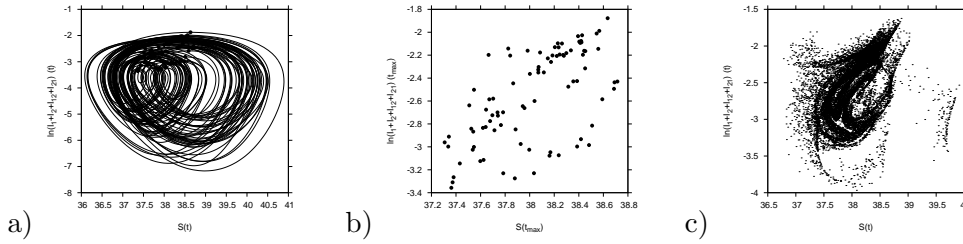


Figure 11: In a), the determined local maxima for the chaotic attractor found for  $\alpha = 2$  and  $\phi = 0.7$  (See Fig. 6 c)). In b), scattered maxima plot for the 500 years of simulation. In c) the map of maxima of the overall infected and the respective values for the susceptibles for a very long simulation, using the same conditions as for Fig 11 b). We observed that even after 200000 years, the dots never come back to the same point. Much more structure than the scatter plot appears. The fingerprint of the chaotic attractor is clearly visible now.

Whereas in Fig. 11 b) we use 500 years of simulations, observing rather erratical scattering of points of local maxima, for Fig. 11 c) we use the local maxima of a long simulation of 200 000 years to observe the clear fingerprint of deterministically chaotic behaviour.

### 3.6 Bifurcation diagrams

Plotting the local maxima of  $\ln(I)$  over the varying parameter  $\phi$ , we obtain a bifurcation diagram, in which fixed points and simple limit cycles appear as one dot per parameter value, whereas double-limit cycles appear as two dots, more complicated limit cycles as more dots, and chaotic attractors as continuously distributed dots for a single  $\phi$  value (see Fig. 12).

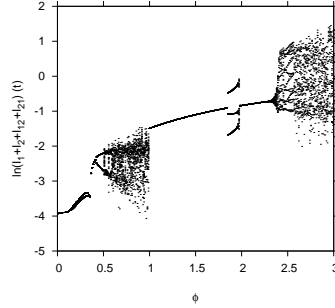


Figure 12: *Bifurcation diagram for the maxima of the overall infected with changing parameter  $\phi$  and  $\alpha = 2$ . We observed a chaotic window for  $\phi < 1$ , region of "inverse ADE", where this dynamical behaviour has never been described before, and another one for  $\phi > 1$ , called by ADE chaotic window, found in previous publications [6, 7].*

To be sure that this unexpected behaviour for  $\phi < 1$  not just appears because of this specific  $\alpha$  value, we look at the robustness of the findings with varying the temporary cross-immunity parameter values.

For  $\alpha = 1$  e.g, both chaotic windows appears, and surprisingly in the region of "inverse ADE" this window is even larger (see Fig. 13).

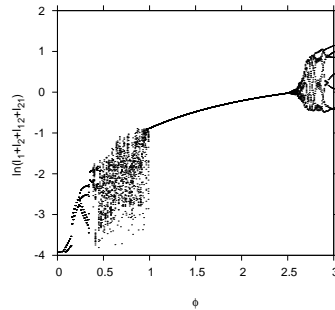


Figure 13: *Bifurcation diagram for the maxima of the overall infected with changing parameter  $\phi$ . Now  $\alpha = 1$ . The bifurcation diagram appears to be quite robust against changes of parameters around the region under investigation.*

Only for very large values of  $\alpha$ , where temporary cross-immunity becomes unimportant due to the low resident times in the classes  $R_1$  and  $R_2$ , the chaos window for  $\phi < 1$  disappears, and then ADE as increasing infectivity on a secondary infection condition seems to be the only mechanism to observe deterministic chaos (see Fig. 14).

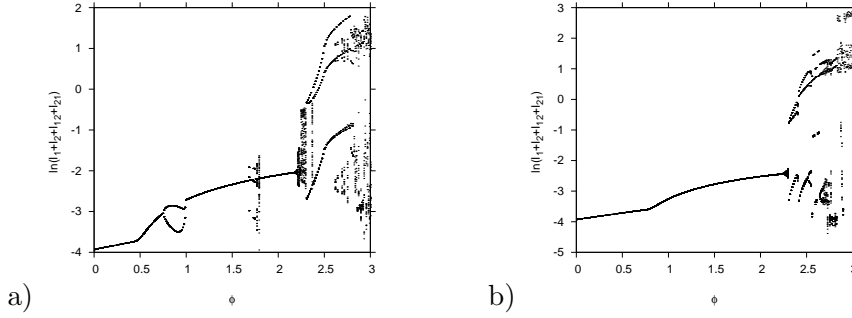


Figure 14: *Bifurcation diagram for the maxima of the overall infected with changing parameter  $\phi$ . Now for a very large value of  $\alpha$  we get close to the models found in the literature, where the temporary cross-immunity is not considered. a) For  $\alpha = 10$ , The chaos window for  $\phi < 1$  disappears completely as the temporary cross-immunity becomes shorter or unimportant. b) For  $\alpha = 20$  it becomes clear that there is no other dynamics in the region for  $\phi < 1$ , than fixed points or simple limit cycles.*

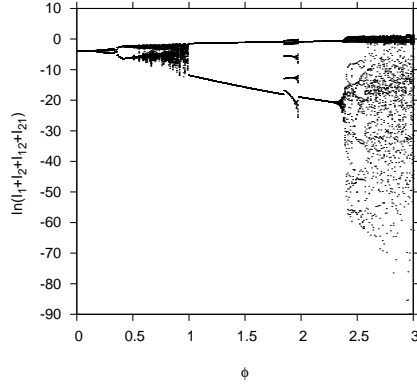


Figure 15: *Bifurcation diagram for the extrema of the overall infected with changing parameter  $\phi$ .  $\alpha = 2$ . For the chaotic window for  $\phi > 1$  the minimal values go to very low numbers of infected.*

Finally, plotting not just the local maxima but also the local minima of  $\ln(I)$  in a bifurcation plot, as done in Fig. 15, we observed again for  $\phi > 1$  very low troughs of infected, whereas in the chaotic region for  $\phi < 1$  the overall number of infected stays always sustainably high.

## 4 Summary

Our analysis shows that also for "inverse ADE", i.e.  $\phi < 1$ , deterministic chaos can be observed, when taking the temporary cross-immunity reported in the medical literature into account.

This indicates that deterministic chaos is much more important in multi-strain models than previously thought. We could show this in a very basic model with only two strains and one reinfection possible, not needing the ADE

mechanism, but rather stating that upon second infection hosts spread a disease less likely, since it might be more harmful. This mechanism could be present in other diseases than dengue fever, hence of much wider interest.

## 5 Acknowledgments

We would like to thank Gabriela Gomes, Lisbon, for valuable discussions on multi-strain dynamics, Francisco Lemos and Sônia Diniz, Belo Horizonte, for valuable information about dengue epidemiology.

## References

- [1] Ruelle, D., & Takens, F. (1971) On the Nature of Turbulence, *Commun. Math. Phys.* **20**, 167–192. See also *Commun. Math. Phys.* **23** (1971), 343–344.
- [2] Ott, E. (1993) *Chaos in Dynamical Systems* (Cambridge University Press, Cambridge).
- [3] Ruelle, D. (1989) *Chaotic Evolution and Strange Attractors* (Cambridge University Press, Cambridge).
- [4] Halstead, S. B. (1982) Immune enhancement of viral infection. Progress in Allergy. *Progress in Allergy*. **31**, 301–64.
- [5] Halstead S. B. (2003) Neutralization and antibody-dependent enhancement of dengue viruses. *Advances in Virus Research*. **60**, 421–67.
- [6] Ferguson, N. et al. (1999) The effect of antibody-dependent enhancement on the transmission dynamics and persistence of multiple-strain pathogens. *Proc. Natl. Acad. Sci.* **96**, 790–94.
- [7] Schwartz, I.B., Shaw, L.B., Cummings, D.A.T., Billings, L., McCrary, M., Burke, D.S. (2005) Chaotic desynchronization of multi-strain diseases. *Physical Review*. **E 72**, 066201–6.
- [8] Wearing, H.J., & Rohani, P. (2006) Ecological and immunological determinants of dengue epidemics, *PNAS* **103**, 11802–11807.
- [9] World Health Organization. (2002) *Dengue and Dengue Hemorrhagic Fever*. (World Health Org., Geneva, Fact Sheet **117**).
- [10] Favier, C. et al. (2005) Influence of spatial heterogeneity on an emerging infectious disease: the case of dengue epidemics. *Proc. Biol. Sci.* **272**, 1171–7.
- [11] Monath T. P. (1994) Dengue: The risk to developed and developing countries. *Proc. Natl. Acad. Sci. U.S.A.* **91**, 2395–2400.
- [12] Rigau-Pérez, J. G. et al. (1998) Dengue and dengue haemorrhagic fever. *The Lancet*. **352**, 971–77.
- [13] Rosen, L. et al. (1983) Transovarial transmission of dengue viruses by mosquitoes: *A. albopictus* and *A. aegypti*. *Am. J. Trop. Med. Hyg.* **32**, 1108–19.

- [14] Mortimer, R. *Aedes aegypti* and Dengue fever. **Access at:**  
<http://www.microscopy-uk.org.uk/mag/art98/aedrol.html>
- [15] Derouich, M., Boutayeb, A., & Twizel, E. H. (2003) A model of dengue fever. *BioMedical Engineering OnLine*. **Access at:**  
<http://www.biomedical-engineering-online.com/content/2/1/4>
- [16] Lei, Huan-Yao. et al. (2001) Immunopathogenesis of Dengue Virus Infection. *Biomedical Science*. **8**, 337–88.
- [17] Francisco Lemos, pers. comm., zoonosis control coordinator of Secretaria de Estado de Saúde de Minas Gerais, Brazil, and S/nia Diniz, pers. comm., responsible of the virology and rickettsioses service from the Fundao Ezequiel Dias, Minas Gerais, Brazil.
- [18] Stephenson, J. R. (2005) Understanding dengue pathogenesis: implications for vaccine design. *Bull. World Health Organ*. **83**, 308–14.
- [19] Fischer, D. B., & Halstead, S. B. (1970) Observations related to pathogenesis of dengue hemorrhagic fever. V. Examination of age specific sequential infection rates using a mathematical model. *J. Biol. Med.* **42**, 329–49.
- [20] Packard, N.H., Crutchfield, J.P., Farmer, J.D. & Shaw, R.S. (1980) Geometry from a Time Series, *Phys. Rev. Lett.* **45**, 712–716 .
- [21] Takens, F. (1981) Detecting strange attractors in turbulence, in: *Dynamical Systems and Turbulence, Warwick 1980* eds. D. Rand, L.S. Young *Lecture Notes in Mathematics* **898** (Springer, Berlin) 366 ff.
- [22] van Kampen, N. G. (1992). *Stochastic Processes in Physics and Chemistry* (North-Holland, Amsterdam).
- [23] Alonso, D., McKane, A., & Pascual, M. (2006) Stochastic Amplification in Epidemics, *Journal of the Royal Society Interface*, FirstCite Early Online Publishing (not yet in paper): DOI: 10.1098/ rsif.2006.0192.
- [24] McKane, A. J. & Newman, T. J. (2005) Predator-prey cycles from resonant amplification of demographic stochasticity, *Phys. Rev. Lett.* **94**, 218102–7.
- [25] Farmer, J.D. & Sidorowich, J.J. (1987) Predicting chaotic time series, *Phys. Rev. Lett.* **95**, 845–848.